Scientific Research Publishing

Journal of Applied Mathematics and Physics, 2022, 10, 1998-2014
https://www.scirp.org/journal/jamp
ISSN Online: 2327-4379
ISSN Print: 2327-4352

A Spherical Atom Model of Helium Based on Well-Defined Electron Trajectories

Thomas Allmendinger

Independent Scholar, Glattbrugg (close to Zurich), Switzerland
Email: inventor@sunrise.ch

How to cite this paper: Allmendinger, T. (2022) A Spherical Atom Model of Helium Based on Well-Defined Electron Trajectories. *Journal of Applied Mathematics and Physics*, **10**, 1998-2014.
https://doi.org/10.4236/jamp.2022.106136

Received: May 2, 2022
Accepted: June 26, 2022
Published: June 29, 2022

Abstract

The present approach is an advancement of the author's former attempts to develop an atom model of Helium with well-defined electron trajectories. Thus it calls in question the traditional quantum mechanics which assume—in contrast and as a consequence of Heisenberg's uncertainty principle—electronic probabilities of presence. Its basic idea consists of the assumption that the motions of the two electrons are influenced by their spins exhibiting the value $h/2\pi$, but in two different ways: on the one hand, one spin induces a rotation; and on the other hand, the other spin induces a harmonic oscillation. A second important relation is given by the fact that the retroactive force of the oscillation process is due to the centrifugal force when the process runs along the surface of a sphere, whereas in usual oscillation processes—such as the one of a spring pendulum—it is due to a permanent shift between potential and kinetic energy. Therefore, in the present case, the potential energy remains constant since the distance between the nucleus and the—diametrically positioned—electrons remains constant. Considering these two conditions and the usual physical relations such as Coulomb attraction, centrifugal force, and the conservation laws of the angular momentum and of the energy, it was possible to compute the respective key values. Thereby, the deflection of the oscillation angle $\psi = 45^\circ$ is remarkable. Finally, the process is described using a Cartesian coordinate system with z as the rotation axis, a variable oscillation distance d and variable rotation velocities r_{rot}. Thereby, the projections onto the x-axis and on the y-axis are not identically equal, leading to an elliptic projection shape. Thus this system is anisotropic, in contrast to the isotropic array of the conventional quantum mechanics according to Schrödinger, where the 1s-orbital is spherically symmetrical. This anisotropy explains the existence of interatomic Van der Waals forces, which enable the condensation of Helium, even though the condensation temperature is very low. But in particular, it exhibits well-defined electron waves, thus finally delivering the explanation of the hypothesis of Louis de Broglie, which

has been established 100 years ago.

Keywords

3D-Atom-Model, Electron-Spin, Electron Wave, Confutation of the Traditional Quantum Mechanics according to Schrödinger and Heisenberg

1. Introduction

The hydrogen atom model of Niels Bohr was published in 1913 [1], and based on Max Planck's quantum theory of light, was published in 1900 [2] and supplemented by Albert Einstein's photoelectric effect in 1905 [3], represented a cardinal milestone in understanding the structure of matter and its relevance for electromagnetic radiation. This atom model could explain the mathematical regularities of the absorption- and emission-lines in the discrete UV-spectrum of hydrogen, first discovered by Balmer already in 1885 [4], and later revealed by Rydberg. The explanation of these regularities is given by assuming definite plane electron orbits around the nucleus, characterized by integer multiples of its angular momentum $h/2\pi$, which is accurate for the ground state. It is worth knowing that Planck's constant h, originally designated as "quantum of action", exhibits the same unit as an angular momentum does, namely Js. However, the real cause for this coincidence and for this multiplicity could not be found. Moreover, the existence of such a ground state (Bohr called it "permanent state") could not be explained, *i.e.,* it was not intelligible why the angular momentum does not fall below the numerical value of $h/2\pi$—as would be expected for a Hertz oscillator. And finally, in Bohr's mathematical model, no frequency of the electron motion appears, which corresponds to the frequency of the absorbed or emitted light (It should be noticed that Bohr's electron orbits correspond to energetically excited electronic states, and not to electron shells, which are commonly assumed for atoms with higher atomic numbers, explaining the "aufbau-principle" of the periodic system, and solely concerning the ground states of the atoms. It is not even possible to describe the Helium atom in terms of Bohr's model).

Ten years later, the hypothesis of Louis de Broglie allowed taking a step forward, assuming a wavy nature of electron trajectories, and implying standing electron waves in the excited states. However, such well-defined trajectories could not be found and depicted. Indeed, even if three-dimensionality is envisaged, it seems impossible to describe a wavy electron motion based on the usual harmonic oscillator where a permanent shift occurs between potential and kinetic energy. A respective approach of the author [5], exhibiting a hyperboloid oscillation of the electron combined with a rotation, was meanwhile abandoned.

As a consequence, Heisenberg postulated the so-called "uncertainty principle", implying for each electron probabilities of presence, instead of well-describable trajectories. This assumption was adopted by the leading physicists, es-

pecially by Born, Schrödinger and Dirac. 100 years later, it still represents the "official" quantum mechanical doctrine, even if it contradicts the fundamental scientific principle of causality, ignoring the existence of angular momentum in the ground state, disregarding the fact that standing waves represent the epitome of accuracy, and hazarding the lacking vividness and unintelligibility of that model. After all, the charge cloud model of Kimball was proposed in 1940 [6], delivering an improved visualisation, qualitatively explaining the atomic structure of the elements as well as the valences in molecular bonds. It is well usable in chemistry, but it does not exactly render the original quantum mechanical approach.

Based on the multiplicities of spectral lines found in the presence of magnetic fields, Uhlenbeck and Goudsmith postulated in 1925 the *electron spin* [7] [8]. This phenomenon was implemented afterwards in the already existing theory, introducing the Pauli-principle. However, it is of extreme importance for the whole quantum mechanical reception since it explains the existence of the basic angular momentum in the Bohr model due to an empirically detectable coupling with the spin of the electron. Hence it must constitute the theory and cannot be added afterwards to a basically insufficient theory. When the spin and its coupling with the electron orbit are regarded from the outset, Heisenberg's uncertainty principle becomes unnecessary and should thus be abandoned.

After having realized the cause for the permanent ground state of the hydrogen atom—namely the electron spin—the author's way was clear for developing a vivid model of the H_2-molecule [9], exhibiting planar electron orbits (**Figure 1**).

Analogously to the conventional method of Heitler and London [10] [11], the bond length was computed by searching the total energy minimum (**Figure 2**).

Since the bond length can be directly determined by X-ray measurements, verification was possible by empirical evidence, delivering an accurate result. In contrast to this, the results of Heitler and London, as well as those of others [12] delivered variable and less accurate results. Thus empiric evidence for the existence of well-defined electron trajectories could be delivered—namely by explaining the ground-state of the H_2-molecule—in contrast to the conventional theory.

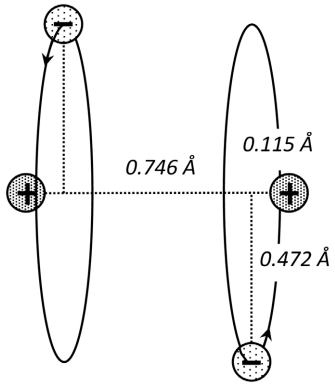

Figure 1. Model of the H_2-molecule (true to scale), according to [9].

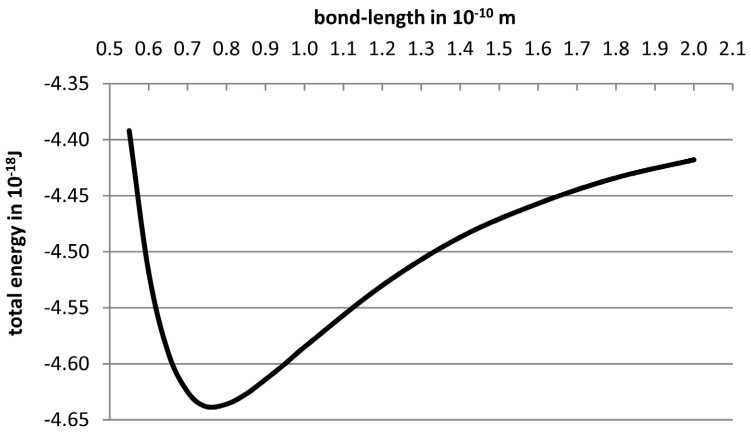

Figure 2. Total energy as a function of the bond-length at the H_2-molecule, according to [9].

Extending this approach, atom models for the noble gases Helium and Neon were developed by the author [13], in particular for Helium. Since a planar array according to **Figure 3** is not permissible because the spins of both electrons would relate in the same manner to the nucleus, thus contradicting the Pauli-principle, an eccentric array according to **Figure 4** was proposed.

In a subsequent publication [14], this model was extended to a rotating rotator, assuming a spherical envelope (**Figure 5**).

However, this assumption turned out to be inaccurate, leading to a revision or rather refutation in [15]. In addition to the therein alleged arguments, this approach of eccentrically rotating electrons has generally to be abandoned since it implicates the lack of a force-equilibrium between the Coulomb attraction and the centrifugal force of the rotating electrons. This becomes also manifest when an energetic consideration is made by minimizing the total energy (*i.e.* the sum of the kinetic and of the potential energy) as a function of the proportion of the two eccentric edges, which yields a planar rotation plane.

In contrast to these model approaches, the here presented model does not exhibit such disadvantages even if it implicates well-defined electron trajectories. It resembles the model of the excited electron state at the hydrogen atom (**Figure 6**), which was recently published by the author [16], and exhibits a spherical envelope, but only to a certain degree, thus describing a sphere segment. Thereby, it explains the existence of intramolecular forces (van der Waals-forces), leading to a condensation point above absolute zero, whereas the conventional orbital theory cannot explain this due to the spherical symmetry of the 1s-orbital.

The idea of the previous model was to allocate a separate rotation to each electron induced by its spin, whereby the two rotations were coupled and orthogonal to one another (**Figure 5**). The error was to equal a rotation with an oscillation. But such an equalisation can only be made with respect to the position of a rotating electron which is projected onto the axis of a corresponding harmonic oscillator since it doesn't describe the real course of an oscillating electron.

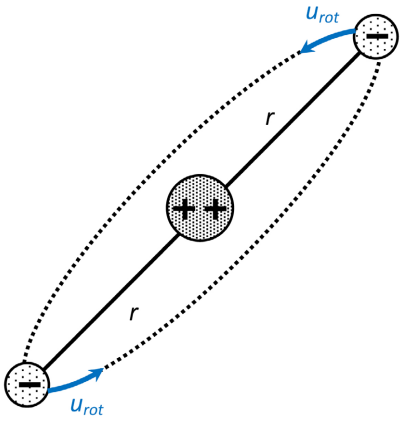

Figure 3. Concentric atom model of Helium.

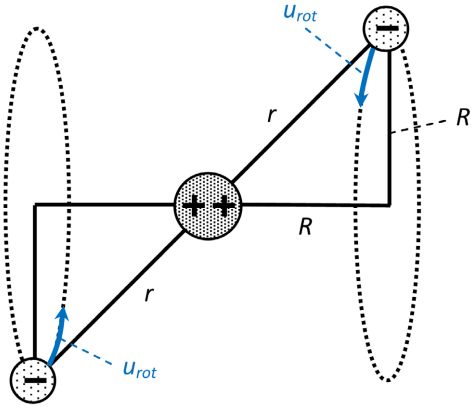

Figure 4. Eccentric double-cone atom model of Helium, according to [13].

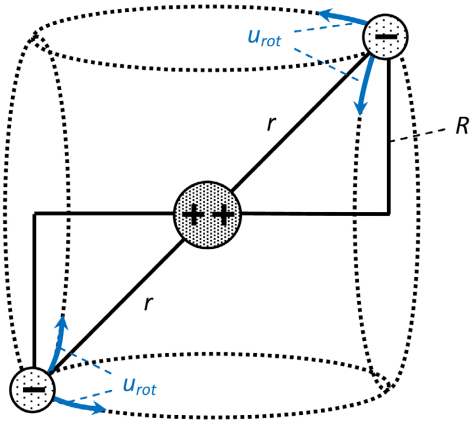

Figure 5. Extended eccentric model of Helium, according to [14].

Instead, the essential idea of the present approach consisted of a combination of a (horizontal) *rotation* with a (vertical) *oscillation*, whereby these two different movements are induced by the spins of the two diametrically positioned electrons. Thus, it is assumed that the spin of an electron cannot only induce a rotation but also an oscillation, whereby the oscillation frequency is identically equal to the frequency of a related rotation frequency.

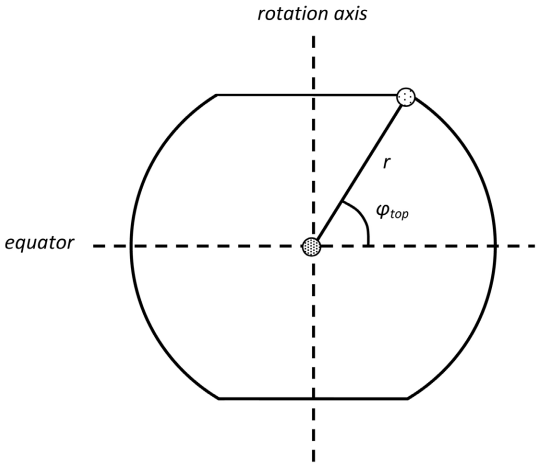

Figure 6. Envelope of the electron trajectory at the first excitation state of the H-atom-model, according to [16].

2. The Elucidation of the Present Model

The present model is depicted in **Figure 7**, exhibiting the constant spherical radius R. Therein, the two diametrically positioned electrons are permanently rotating around the oscillating axe at a variable distance d between two top positions d_{top}, passing an intermediate position (designated as equator). Their oscillating velocity is designated as u_{osc}. It amounts zero at the top positions and maximal at the equator position ($=u_{osc,eq}$). Since the angular momentum of the rotating electrons must be constant, namely $h/2\pi$, and since the rotation radius r_{rot} varies, the rotation velocity varies, too, being larger at the top position than at the equator position. But its total velocity is nevertheless larger at the equator position due to their oscillation component, whereby $(u_{tot})^2 = (u_{rot})^2 + (u_{osc})^2$. The *retroactive force* arises from the different rotation radii, implicating different rotation velocities at different positions and different tangential forces F_{tang}, acting reactively. The fact that this oscillating effect bewilderingly fulfils the law of a harmonic oscillator will be formally demonstrated below.

The horizontally running *rotation process* is formally described by the relation

$$\varphi = \omega \cdot t \tag{1}$$

whereby φ = rotation angle and ω = (constant) angular velocity.

The vertically running *oscillation process* is described by the relation

$$d = d_{top} \cdot \sin(\omega t) \tag{2}$$

whereby d = oscillation distance, and d_{top} = amplitude.

The oscillation velocity u_{osc} can be calculated by differentiation:

$$u_{osc} = \dot{d} = d_{top} \cdot \omega \cdot \cos(\omega t) \tag{3}$$

(Remark: Here the velocities are generally abbreviated with u in order to avoid confusion with the frequency υ).

As a consequence, the retroacting force F_{osc} is given by the relation

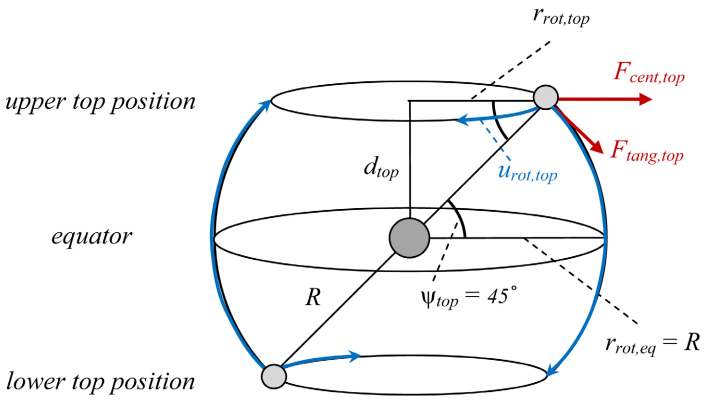

Figure 7. Depiction of the present atom model of Helium at the top positions of the electrons.

$$F_{osc} = \ddot{d} \cdot m_e = -m_e \cdot d_{top} \cdot \omega^2 \cdot \sin(\omega t) = -d \cdot m_e \cdot \omega^2 \tag{4}$$

where m_e = electron mass.

Moreover, the centrifugal force F_{cent} acts an important part. It is given by the relation

$$F_{cent} = m_e \frac{u_{rot}^2}{r_{rot}} \tag{5}$$

And finally, the spin-orbit coupling has to be considered, yielding the expression for the orbital angular momentum

$$L_e = u_{rot} \cdot r_{rot} \cdot m_e = h/2\pi \tag{6}$$

with h = Planck's constant.

It goes without saying that the positions of the two electrons must be twisted by 180˚. Moreover, the equilibrium between the Coulomb-force and the centrifugal force has to be regarded, analogously to Bohr's approach, but considering the interference of the Coulomb forces between the three involved particles. This will be discussed in the next chapter.

The spherical course of the vertical electron movement generates an oscillating effect when the two electrons are horizontally rotating around the oscillating axis. Based on the vector diagram of **Figure 8**, evidence can be formally provided that this oscillating effect fulfils the law of a harmonic oscillator.

Thereof, the following relations are evident:

$$F_{tang} / F_{cent} = \sin\psi \tag{7}$$

$$F_{osc} / F_{tang} = \cos\psi \tag{8}$$

$$r_{rot} / R = \cos\psi \tag{9}$$

$$d/R = \sin\psi \tag{10}$$

Combined with Equation (5), for F_{osc} the following relation is obtained:

$$F_{osc} = d \cdot m_e \cdot \frac{u_{rot}^2}{R^2} \tag{11}$$

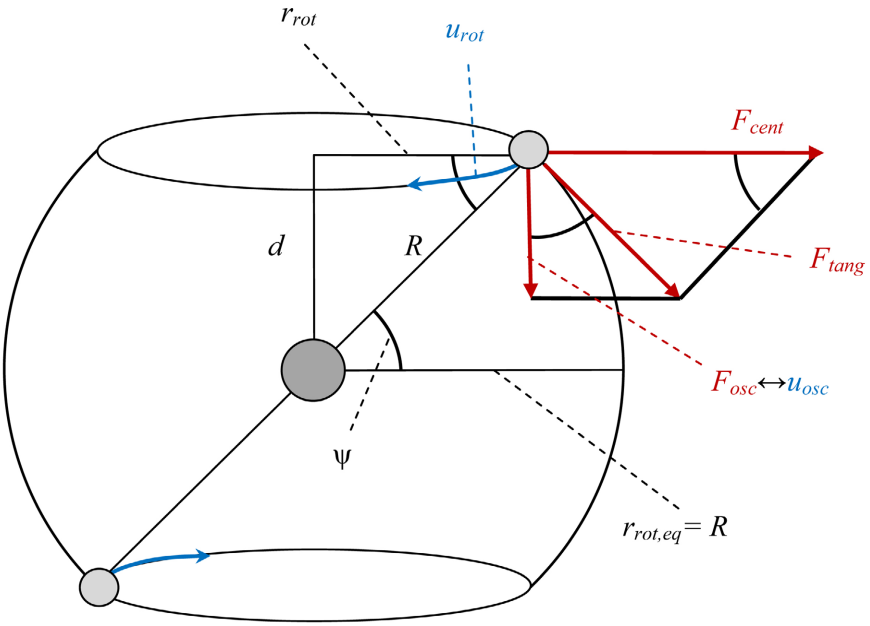

Figure 8. Vector diagram relating to the centrifugal force F_{cent}.

At first view, therein no direct dependency of d is obvious. However, by replacing one of the u_{rot}-factors by the relation

$$u_{rot} = \omega \cdot r_{rot} \tag{12}$$

and by regarding Equation (6), the relation (13) is obtained, which expresses a direct proportion between the oscillation distance d and the reversing force F_{osc}, what is characteristic for a harmonic oscillator:

$$F_{osc} = d \cdot \frac{h}{2\pi} \cdot \frac{\omega}{R^2} \tag{13}$$

3. The Computation of the Key Values

In order to mathematically describe the model system, it is necessary to evaluate the key values R, $r_{rot,eq}$, $r_{rot,top}$, $u_{rot,eq}$, $u_{rot,top}$, d_{top} and ω. Thereto, the above established relations may be used. Moreover, an expression for the interference of the Coulomb-forces has to be deduced. And finally, a connection between the two processes has to be found. This is easily possible by making the hypothetical assumption $\boldsymbol{u_{osc,eq} = u_{rot,eq}}$.

The numerical values of the involved natural constants are assumed as follows:

$$m_e = 9.1093819 \times 10^{-31}\ \text{kg} \quad \text{(mass of the electron)}$$

$$K = e^2 / 4\pi\varepsilon_0 = 2.307 \times 10^{-28}\ \text{J} \cdot \text{m}$$

$$h/2\pi = 1.0545716 \times 10^{-34}\ \text{J} \cdot \text{s}$$

The interference of the Coulomb-forces between the two electrons and the nucleus (whose electrical load is 2+) is scheduled in **Figure 9**:

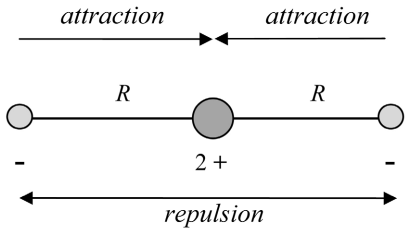

Figure 9. Interference of the Coulomb forces in a two-electron system.

Thereby, each of the two attraction forces amounts to $2K/R^2$, whereas the repulsion between the two electrons amounts to $-K/4R^2$. When the interference is focussed onto the nucleus, the relative attraction is

$$F_{Coul} = \frac{\frac{2\cdot 2K}{R^2} - \frac{K}{4R^2}}{2} = \frac{15K}{8R^2} \tag{14}$$

where $R = r_{rot,eq}$ = distance nucleus-electrons.

Based on these relations, the following derivations are possible:

At the equator, there is equilibrium between the Coulomb-force (14) and the centrifugal force. However, that centrifugal force cannot be expressed by Formula (5) since not only the rotation velocity is relevant, but also the oscillation velocity which is identically equal with the rotation velocity. Moreover, at this position r_{rot} becomes equal to R. Hence

$$\begin{aligned} F_{cent,eq} &= m_e \cdot \left(u_{tot,eq}\right)^2 \Big/ r_{rot,eq} \\ &= m_e \cdot \left[\left(u_{rot,eq}\right)^2 + \left(u_{osc,eq}\right)^2\right] \Big/ r_{rot,eq} \\ &= 2m_e \cdot \left(u_{rot,eq}\right)^2 \Big/ r_{rot,eq} \end{aligned} \tag{15}$$

The equalization of (14) and (15) yields

$$15K/16r_{rot,eq} = m_e \cdot \left(u_{rot,eq}\right)^2 \tag{16}$$

Now, relation (6)—concerning the angular momentum—can be implemented, delivering the result

$$u_{rot,eq} = (15/16)\cdot K \cdot 2\pi/h = 2.0509\times 10^6 \text{ m/s} \tag{17}$$

Combined with (6) or with (16), this value of $u_{rot,eq}$ yields

$$r_{rot,eq} = R = 0.56448\times 10^{-10} \text{ m} \tag{18}$$

Since the law of conservation of energy must be fulfilled, and since the potential energy remains constant due to the constant R, the kinetic energy at the equator must be equal to the kinetic energy at the top position of the electrons. Thereby it must be considered that the total kinetic energy is double the amount of the kinetic energy of one electron.

$$\begin{aligned} &E_{kin,eq} = 2\cdot(1/2)\cdot m_e \cdot \left(u_{tot,eq}\right)^2 = 2m_e \cdot \left(u_{rot,eq}\right)^2 = E_{kin,top} = m_e \cdot \left(u_{rot,top}\right)^2 \\ &\rightarrow u_{rot,top} = \sqrt{2}\cdot u_{rot,eq} = 2.900\times 10^6 \text{ m/s} \end{aligned} \tag{19}$$

According to this, the **kinetic energy** amounts to **7.661 × 10^{-18} J**. On the other hand, the **potential energy** of the two electrons is given by the expression

$$E_{pot} = -2 \times 2K/R = -16.358 \times 10^{-18} \text{ J}.$$

Since according to (6)

$$u_{rot,top} \cdot r_{rot,top} = u_{rot,eq} \cdot r_{rot,eq}$$

$$\rightarrow r_{rot,top} = r_{rot,eq} \cdot u_{rot,eq} / u_{rot,top} = r_{rot,eq} / \sqrt{2} = R/\sqrt{2} = 0.3990 \times 10^{-10} \text{ m} \quad (20)$$

As obvious in Figure 7, according to the Theorem of Pythagoras

$$\left(d_{top}\right)^2 = R^2 - \left(r_{rot,top}\right)^2$$

$$\rightarrow d_{top} = 0.3990 \times 10^{-10} \text{ m} = r_{rot,top} \quad (21)$$

and

$$\psi_{top} = 45^\circ \quad (22)$$

Finally, Equation (3) delivers the relation for ω, namely

$$u_{osc,eq} = u_{rot,eq} = d_{top} \cdot \omega \rightarrow \omega = \frac{u_{rot,eq}}{d_{top}} = 5.140 \times 10^{16} \text{ s}^{-1} \quad (23)$$

$$\rightarrow \text{frequency } \upsilon = \omega/2\pi = 0.818 \times 10^{16} \text{ s}^{-1}$$

4. The Graphic Representation of the Model

In order to render the courses of the relevant variables using Excel of Microsoft, the Cartesian coordinates have to be evaluated. Preferably, they should be visually compatible with the array in Figure 7. Hence, the axes were arranged according to Figure 10. Thereby, the (vertical) z-axis represents on the one hand the rotation axis, and on the other hand the axis along which the harmonic oscillation runs. Moreover, it has to be regarded that the rotation radius r_{rot} is not constant but varies dependent on the oscillating distance d (which is identical with z).

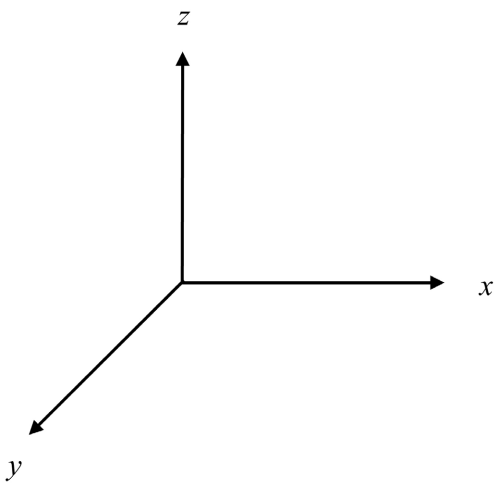

Figure 10. Arrangement of the axes in the present Cartesian coordinate system.

The x- and the y-axis can be described by the following trigonometric functions:

$$x = r_{rot} \cdot \sin\varphi \tag{24}$$

and

$$y = r_{rot} \cdot \cos\varphi \tag{25}$$

where by r_{rot} = rotation radius, φ = rotation angle = ωt, and ω = angular velocity = constant.

On the other hand, the Cartesian coordinate of the oscillation process is given by the relation

$$z = d = d_{top} \cdot \sin\varphi \quad \text{cf. (2)}$$

whereby d = oscillation distance, and d_{top} = amplitude.

d_{top} has been calculated (21), exhibiting the value of 0.3990×10^{-10} m.

Using this value, z can be computed as a function of φ according to Equation (2).

Furthermore, from Figure 8 is evident—according to the Theorem of Pythagoras—

$$\left(r_{rot}\right)^2 = R^2 - d^2 \tag{26}$$

whereby

$$R = 0.56448 \times 10^{-10} \text{ m} \quad \text{cf. (18)}$$

The respective square root yields the value of r_{rot} as a function of φ.

Finally, u_{tot} can be determined by considering the relation

$$\left(u_{tot}\right)^2 = \left(u_{rot}\right)^2 + \left(u_{osc}\right)^2 \tag{27}$$

Thereto, the value of u_{rot} is given by Equation (12) with $\omega = 5.140 \times 10^{16}$ s^{-1}, and the one of u_{osc} by Equation (3), thus

$$\left(u_{tot}\right)^2 = \omega^2 \cdot \left[\left(r_{rot}\right)^2 + \left(d_{top}\right)^2 \cdot \cos^2\varphi\right]$$

whereby $(r_{rot})^2$ can be determined by Equation (26).

The following diagrams are solely related to one electron, except the diagram in Figure 12 where both electrons are considered, designated by the indices 1 and 2. Thereby, $\varphi_2 = \varphi_1 + 180^\circ$.

In Figure 11, the rotation radius r_{rot} and the oscillation distance d is plotted as a function of the rotation angle φ. As obvious, the course of the electrons is wave-like, whereby the frequency of the rotation radius is twice as much as the frequency of the oscillation distance.

In Figure 12 the x- and the y-intercepts (*i.e.* the projection of the y-value of the electron position onto the x- and the y-axes) are plotted versus φ. Thereby, the wave-like character of the electron movements is demonstrated, too.

In Figure 13 the total velocity u_{tot} is plotted versus φ. Thereby, the wave-like character is manifested even more distinctly.

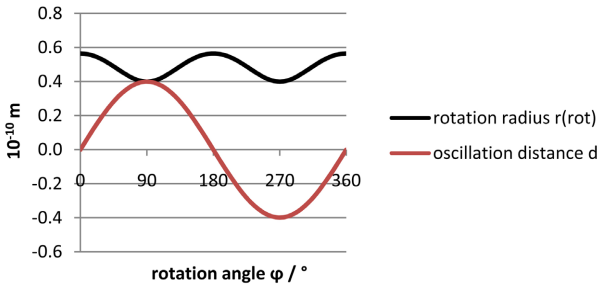

Figure 11. Plots of r_{rot} and d as versus the rotation angle $\varphi = \omega t$.

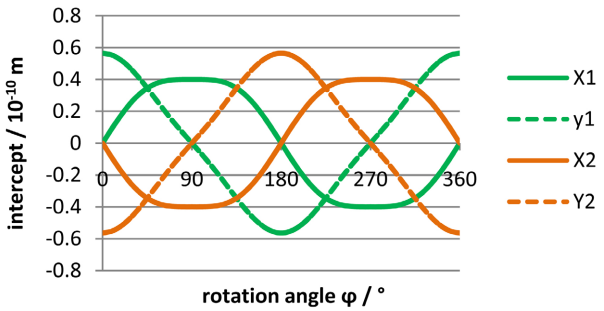

Figure 12. Plots of the x- and the y-intercepts versus φ.

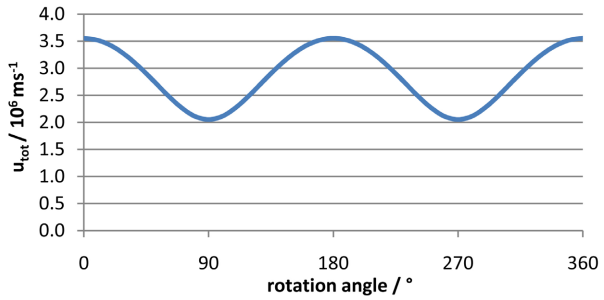

Figure 13. Plot of the total electron velocity u_{tot} versus φ.

In **Figure 14**, the y-intercepts are plotted versus the x-intercepts, due to the variation of φ. The difference of their maximal values is obvious when **Figure 7** is considered: On the top-positions, the y-values are zero, whereas the x-intercepts match +/− $r_{rot,top}$ which is smaller than $r_{rot,eq} = R$. Inversely, on the equator positions the x-values are zero, whereas the y-intercepts are maximal, namely R.

In **Figure 15** and in **Figure 16**, the x- and the y-intercepts are plotted against the oscillating distance d. The significant difference in their shapes is due to the fact that the x- and the y-values are not equivalent because of their anisotropic constellation. However, within these projections in the **Figures 14-16** the wave-like character of the electron movement is not simply obvious.

The electron movement is more vividly manifested by the freeze images of a 3D-animation which are shown the **Figures 17-20**, representing four different camera positions. But therein the wave-like character is also hidden, *i.e.* not easily obvious.

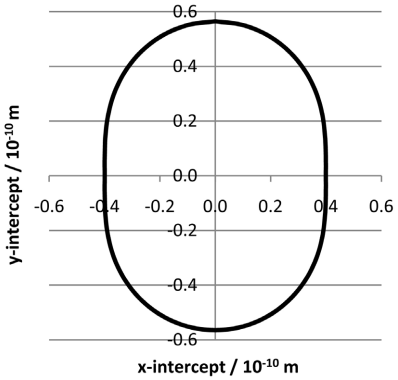

Figure 14. Plot of the *y*-intercepts versus the *x*-intercepts.

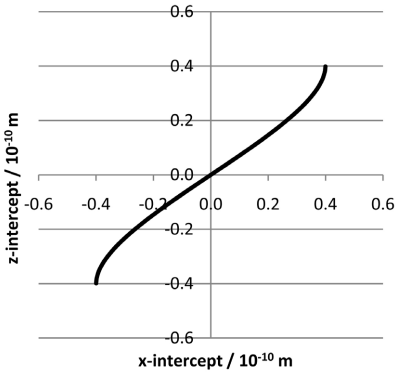

Figure 15. Plot of the *z*-intercepts versus the *x*-intercepts.

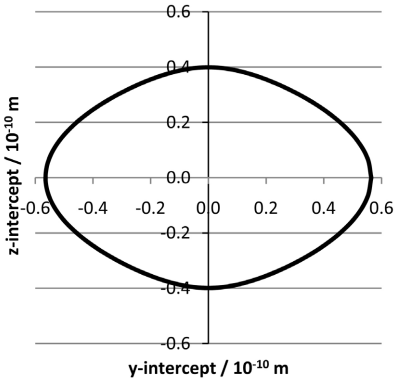

Figure 16. Plot of the *z*-intercepts versus the *y*-intercepts.

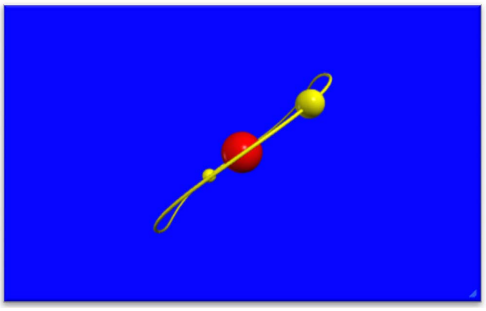

Figure 17. Freeze image of the 3D-animation.

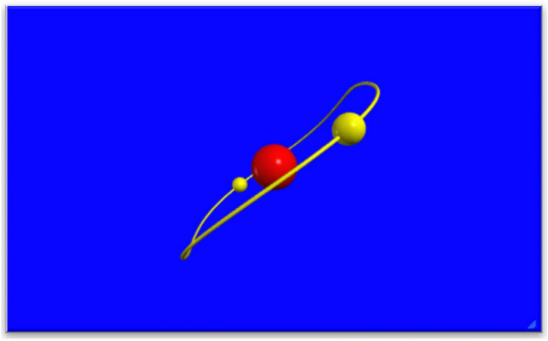

Figure 18. Freeze image of the 3D-animation.

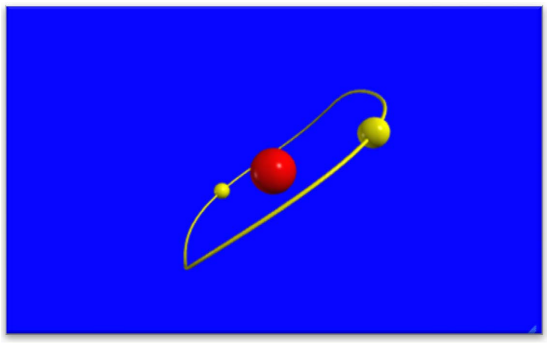

Figure 19. Freeze image of the 3D-animation.

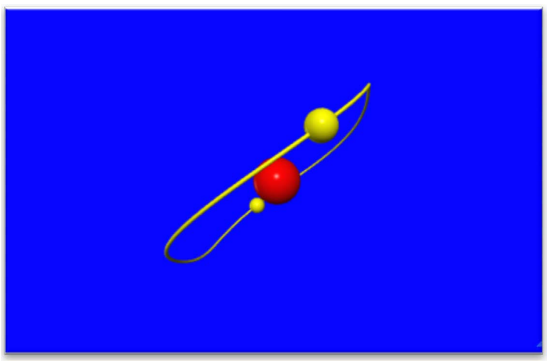

Figure 20. Freeze image of the 3D-animation.

5. Summary and Conclusions

The basic idea of the present approach for the atom model of Helium, comprising well-defined electron trajectories, consists of the assumption that the motions of the two electrons are influenced by their spins exhibiting the value $h/2\pi$, but in two different ways: on the one hand, one spin induces a rotation; and on the other hand, the other spin induces a harmonic oscillation. Both motions can be expressed by sinus- and cosine-functions with the variable $\varphi = \omega \cdot t$ where φ represents the rotation angle, and ω the angular velocity, which is identically equal for both processes. Thereby a vertical axis serves on the one hand as the rotation axis, and on the other hand as the axis along which the oscillation runs between the two top positions and the equator position.

A second important relation is given by the fact that the retroactive force of the oscillation process is due to the centrifugal force when the process runs along the surface of a sphere, whereas in usual oscillation processes—such as the one of a spring pendulum—it is due to a permanent shift between potential and kinetic energy. Therefore, in the present case, the potential energy remains constant since the distance between the nucleus and the—diametrically positioned—electrons remains constant.

Considering these two conditions and the usual physical relations such as Coulomb attraction, centrifugal force, and the conservation laws of the angular momentum and of the energy, it was possible to compute the respective key values. Thereby, the deflection of the oscillation angle $\psi = 45^\circ$ is remarkable.

Lastly, the process is described in a Cartesian coordinate system with z as the rotation axis, a variable oscillation distance d and variable rotation velocities r_{rot}. Thereby, the projections onto the x-axis and on the y-axis are not identically equal, leading to an elliptic projection shape. Thus, this system is anisotropic, in contrast to the isotropic array of the traditional quantum mechanics according to Schrödinger, where the 1s-orbital is spherically symmetrical. This anisotropy explains the existence of interatomic Van der Waals forces which enable the condensation of Helium, even if the condensation temperature is very low.

But in particular, it exhibits well-defined electron waves, thus calling in question the traditional quantum mechanics which assume—in contrast and as a consequence of Heisenberg's uncertainty principle—electronic probabilities of presence, and finally delivering the explanation of the hypothesis of Louis de Broglie which has been established 100 years ago.

However, the wave-like character of the electron movements is not simply evident with respect to the projections on the axes. Moreover, the course of the electron along a spherical surface is not readily obvious, rather appearing as an inclined and nearly planar rotation plane. That is also the case when the freeze images are regarded, which are taken from a 3D animation. But besides the revealed correlations, it should be realized that the atoms are not isolated but rotating due to thermal movement in a gas taking random positions.

It seems not easy to find empirical evidence for this model. Besides the already mentioned existence of a condensation point—which appears difficult to be calculated—the author's observed absorption and emission of IR-light radiation by gases such as Helium [17] promises insofar to deliver evidence for this model as an excited metastable status may be assumed in the form of an electronic pulsation, fulfilling the condition of a standing wave, whose frequency must be equal to the frequency of adsorbed or emitted radiation. But that will be the subject of the following study.

Acknowledgements

I thank David Kummer for performing the 3D animation and the respective freeze images.

Conflicts of Interest

The author declares no conflicts of interest regarding the publication of this paper.

References

[1] Bohr, N. (1913) On the Constitution of Atoms and Molecules. *Philosophical Magazine and Journal of Science*, **26**, 1-25. https://doi.org/10.1080/14786441308634955

[2] Planck, M. (1900) Ueber irreversible Strahlungsvorgänge. *Annals of Physics*, **306**, 69-116. https://doi.org/10.1002/andp.19003060105

[3] Einstein, A. (1905) Ueber einen die Erzeugung und Verwandlung des Lichts betreffenden heuristischen Gesichtspunkt. *Annalen der Physik*, **322**, 132-148. https://doi.org/10.1002/andp.19053220607

[4] Balmer, J.J. (1885) Notiz über die Spectrallinien des Wasserstoffs. *Annalen der Physik und Chemie*, **25**, 80-87. https://doi.org/10.1002/andp.18852610506

[5] Allmendinger, T. (2016) A Classical Approach to the De Broglie-Wave Based on Bohr's H-Atom-Model. *International Journal of Applied Mathematics and Theoretical Physics*, **2**, 1-15. http://www.sciencepublishinggroup.com/journal/paperinfo?journalid=322&doi=10.11648/j.ijamtp.20160201.11

[6] Kimball, G.E. (1940) Directed Valence. *The Journal of Physical Chemistry*, **8**, 188. https://doi.org/10.1063/1.1750628

[7] Uhlenbeck, G.E. and Goudsmith, S. (1925) Ersetzung der Hypothese vom unmechanischen Zwang durch eine Forderung bezüglich des inneren Verhaltens jedes einzelnen Elektrons. *Naturwissenschaften*, **13**, 953. https://doi.org/10.1007/BF01558878

[8] Uhlenbeck, G.E. and Goudsmith, S. (1926) Spinning Electrons and the Structure of Spectra. *Nature*, **117**, 264-265. https://doi.org/10.1038/117264a0

[9] Allmendinger, T. (2018) The Elucidation of the Ground State in the H-Atom-Model of Niels Bohr and Its Application on the Bond-Length Computation in the H_2-Molecule. *International Journal of Molecular and Theoretical Physics*, **2**, 1-10. https://symbiosisonlinepublishing.com/molecular-theoretical-physics/molecular-theoretical-physics09.pdf https://doi.org/10.15226/2576-4934/2/1/00109

[10] Heitler, W. and London, F. (1927) Wechselwirkung neutraler Atome und homöopolare Bindung nach der Quantenmechanik. *Zeitschrift für Physik*, **44**, 455-472. https://doi.org/10.1007/BF01397394

[11] Heitler, W. (1961) Elementare Wellenmechanik. Friedr. Vieweg & Sohn, Braunschweig.

[12] Haken, H. und Wolf, H.C. (2006) Molekülphysik und Quantenchemie. Springer, Berlin, 6. Aufl.

[13] Allmendinger, T. (2018) The Atom Model of Helium and of Neon Based on the Theorem of Niels Bohr. *Journal of Applied Mathematics and Physics*, **6**, 1290-1300. https://www.scirp.org/Journal/PaperInformation.aspx?PaperID=85615 https://doi.org/10.4236/jamp.2018.66108

[14] Allmendinger, T. (2018) The Spherical Atom Model of Helium Based on the Theorem of Niels Bohr. *Journal of Applied Mathematics and Physics*, **7**, 172-180. https://file.scirp.org/Html/15-1721414_90090.htm

https://doi.org/10.4236/jamp.2019.71015

[15] Allmendinger, T. (2019) The Revision of the Alleged Spherical Atom Model of Helium. *Journal of Applied Mathematics and Physics*, **7**, 1212-1219.
https://file.scirp.org/Html/14-1721514_92767.htm
https://doi.org/10.4236/jamp.2019.75081

[16] Allmendinger, T. (2019) A Hydrogen Atom Model with Well-Defined Electron Trajectories. *International Journal of Quantum Foundations/IJQF Supplement* (*Quantum Speculations*), **2**, 1-26.

[17] Allmendinger, T. (2016) The Thermal Behaviour of Gases under the Influence of Infrared-Radiation. *The International Journal of Physical Sciences*, **11**, 183-205.
https://academicjournals.org/journal/IJPS/article-full-text-pdf/E00ABBF60017
https://doi.org/10.5897/IJPS2016.4500